



NMR Single-Pulse Echo in Magnets: Fundamental Formation Mechanisms and Potential Applications for Operation of Spin-echo Processors

G. I. Mamniashvili & T. O. Gegechkori

1. Andronikashvili Institute of Physics, Tbilisi State University, 6 Tamarashvili St., Tbilisi 0179, Georgia

Abstract: The fundamental mechanisms of single-pulse echo formation in magnets were investigated using lithium ferrite and cobalt as examples. The properties of a single-pulse echo and its secondary signals, as well as the secondary signals of a two-pulse echo of ^{57}Fe nuclei in lithium ferrite, were studied and compared with those in cobalt. The experimental results indicate the efficiency of the multiple-pulse mechanism of single-pulse echo formation and its secondary signals in lithium ferrite, as well as in cobalt at low powers of radio-frequency pulses. At radio-frequency powers above a certain threshold value, the single-pulse echo in cobalt is formed through the distortion mechanism of the radio-frequency pulse. A potential application of NMR spin-phenomenon for operation of spin-echo processors was discussed.

INTRODUCTION

The phenomenon of a single-pulse echo (SPE) in spin systems was first observed by Bloom [1] soon after Hahn discovered the effect of a two-pulse nuclear spin echo (TPE) [2]. Bloom also revealed the possibility of an enhancement of the echo in cases where the repetition period of radio-frequency (RF) pulses becomes shorter than the characteristic relaxation times of the spin system under consideration.

The SPE effect was observed only in systems with large Larmor inhomogeneous broadening of the NMR line, when the width of the NMR line is much greater than the Rabi frequency (the amplitude of the RF pulse in frequency units). The SPE signals in such systems had a characteristic “two-hump” shape. Similar SPE signals of ^{59}Co nuclei were observed in ferromagnetic cobalt [3].

However, the numerical integration of Bloom’s equations of motion [1], performed in [3], did not reveal an SPE effect. Later theoretical models that considered only strong Larmor inhomogeneous broadening also did not agree with the experimentally observed SPE signals, leading instead to the formation of an oscillatory free-induction decay (OFID) [4,5].

Interest in the investigation of the SPE phenomenon increased after 1974, when this phenomenon was observed in weakly anisotropic magnets such as MnCo_3 and CsMnF_3 [6]. In these crystals, coupling between the vibrations of the paramagnetic nuclear and the ordered electron subsystems arises at low temperatures, leading to a characteristic repulsion of resonance frequencies (a dynamic NMR frequency shift, DFS).

In this case, the NMR frequency depends on the amplitude of vibrations in the nuclear spin system, which is typical of nonlinear systems. Under such conditions, the traditional Hahn mechanism becomes ineffective, and the nuclear spin echo is formed via a frequency-modulation (FM) mechanism. One of the essential distinctive features of this mechanism is

the possibility of non-resonant excitation of the echo (in addition to the usual resonance mechanism), when the frequency of the RF pulse differs from the NMR frequencies of the excited spins by a value greater than the width of the NMR line.

In terms of the FM mechanism, the SPE and its secondary-echo signals observed in systems with a strong dynamic frequency shift can naturally be explained.

In 1979, Chekmarev et al. suggested the first theoretical mechanism for the formation of SPE in Hahn's systems—the non-resonant mechanism [7]. In this case, the nonadiabatic switching on of an RF field leads to the appearance of an angle between the equilibrium direction of the nuclear magnetization and the direction of the effective field H_{ef} in the rotating coordinate system (RCS), and then to the precession of isochromates about H_{eff} . A switching off of the RF field causes their phase interchange and the formation of SPE signals. The cause of the appearance of SPE in this case is the ellipticity of the projection of the trajectory of the nuclear-magnetization vector motion in the rotating coordinate system onto the transverse plane during the action of the exciting RF pulse (this ellipticity is due to the inclination of the precession axis relative to the axis).

There also exists another viewpoint on the process of SPE formation under non-resonant excitation. It was shown in [8] that under conditions of non-resonant excitation, the observation of SPE can be related to the fact that the edges of the exciting RF pulse are sufficiently steep, which determines a noticeable spectral density of the RF pulse at frequencies far from the carrier frequency. For this reason, SPE is sometimes called the edge echo, and it is assumed that in the case of single-pulse excitation the rising and trailing fronts of the RF pulse play the role of the two resonance-exciting RF pulses in Hahn's method. Correspondingly, in what follows we will speak of the edge and non-edge mechanisms of SPE formation.

In [9], one more mechanism of SPE formation was considered; this is the so-called distortion mechanism. In this case, the SPE signal arises upon the resonant action of an RF pulse, and the change in the direction of H_{eff} at the fronts of the RF pulse required for the formation of the echo signal arises due to transient processes in radio-frequency circuits. The formation of the SPE signal in the distortion model is explained by the fact that the effect of pulse edges on the sample is close to the action of two individual resonant RF pulses. From this viewpoint, the process of SPE formation closely resembles the formation of the TPE signal by Hahn's mechanism.

For example, the distortion mechanism satisfactorily describes the properties of SPE upon resonant excitation in polycrystalline films, thin foils, and polycrystalline powder of cobalt at helium temperatures [9]. In work [10], the effect of a low-frequency (LF) field on the role of the fronts of RF pulses in the SPE technique was studied. As objects, metallic hexagonal cobalt and lithium ferrite were used. This choice was made because the intensity of the SPE signal in lithium ferrite was much weaker, despite comparable intensities of the TPE signals in these materials.

It was established that the fronts of the SPE pulse in cobalt play the role of two resonant RF signals, since modulation of the envelope of the decaying SPE signal was observed when the duration of the RF pulse increased. This effect was similar to that characteristic of the TPE signal in cobalt in accordance with [9]. No such effect of SPE modulation was observed in lithium ferrite, although the effect of TPE modulation in this magnet was even more intense than in cobalt. On this basis, a conclusion was made about

the possibility of a non-edge mechanism of SPE formation in lithium ferrite, in which the SPE signal is determined by the dynamics of the spin system during the entire duration of the resonant RF pulse.

However, the mechanism of SPE formation in lithium ferrite was not completely understood in that work and was further investigated in [11].

It was shown that the SPE signal in lithium ferrite is formed via a new non-edge mechanism of SPE formation in magnets. This mechanism had previously been studied theoretically and experimentally for several multidomain ferromagnets ([12]) and is known as the multiple-pulse mechanism of SPE formation. It was also demonstrated that the same mechanism is responsible for the formation of secondary SPE and TPE signals in lithium ferrite. These results may also be useful for explaining the nature of secondary SPE and TPE signals observed in other magnets that cannot be adequately described within the framework of existing models [13].

It should be emphasized that understanding the nature of this phenomenon is important not only from a theoretical standpoint but also for practical applications in radio-frequency devices employing the spin-echo effect in magnetic materials [14]. Lithium ferrite is considered a promising material for such devices because it exhibits some of the longest transverse relaxation times among multidomain magnetic systems [15].

In this work, we present the results of experimental and theoretical investigations of the fundamental mechanisms responsible for SPE and TPE formation in lithium ferrite and cobalt.

A potential application of single-pulse spin-echo phenomenon for operation of NMR spin-echo processors is also discussed.

EXPERIMENTAL RESULTS AND DISCUSSION

The experimental setup is shown in Figure 1.

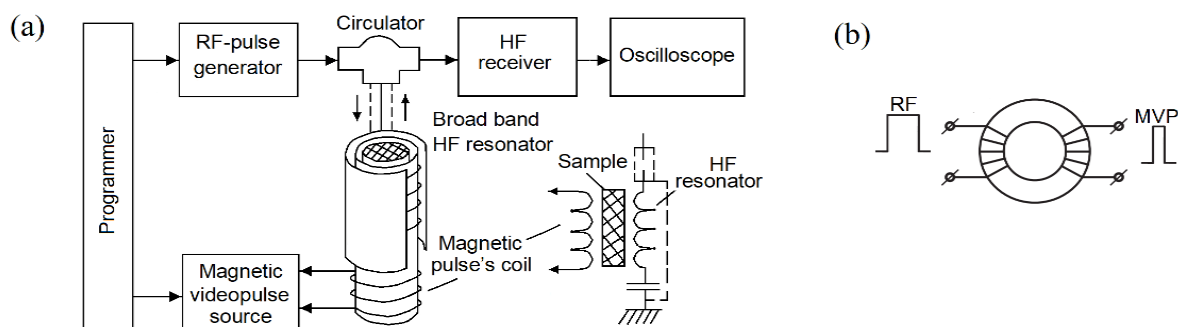


Figure 1: (a) Schematic diagram of the experiment. (b) NMR cell used for measurements on lithium ferrite.

The measurements were carried out using a phase-incoherent spin-echo spectrometer operating in the frequency range 40-400 MHz at a temperature of 77 K. In the frequency range 40-220 MHz, a standard self-excited generator was employed. The oscillator frequency could be smoothly tuned using various inductors and tuning capacitors. In the

200-400 MHz range, a commercial Lecher-type generator was used with a two-wire transmission line containing two inductors with different numbers of turns.

For RF pulse durations ranging from 0.1 to 50 μs , the maximum RF field amplitude at the sample was approximately 3.0 Oe, while the rise time of the pulse fronts did not exceed 0.15 μs . The receiver dead time was approximately 1 μs .

The scheme of the experiment involving pulsed magnetic-field excitation is shown in Figure 4. The pulsed magnetic field was generated by a gated current stabilizer with adjustable amplitude together with an additional copper coil. This arrangement allowed magnetic-field pulses with amplitudes up to approximately 500 Oe to be produced at the sample, which had a characteristic size of about 10 mm.

A detailed description of the NMR spectrometer and the magnetic video-pulse (MVP) unit is given in [16,17]. The amplitude of the echo signal was measured both in the presence and in the absence of the MVP field with amplitude H_d .

The samples used in the experiments were lithium-zinc ferrite $\text{Li}_{0.5}\text{Fe}_{1.0}\text{Zn}_{0.15}\text{O}_4$ rings with diameters of 12-15 mm and a mass of 5.8 g. The samples were enriched with the ^{57}Fe isotope to 96.8% in order to enhance the intensity of the NMR echo signal. In addition, polycrystalline cobalt powders were used. These were prepared by fusion in an inductive furnace and had an average grain size of less than 50 μm [17].

The resonance system of the spectrometer used for ^{57}Fe NMR measurements was similar to that described in [18]. Experimental conditions were optimized to maximize the intensity of the signals under study.

Figures 2 and 3 show representative oscillograms of the single-pulse echo (SPE) and two-pulse echo (TPE) signals, along with their secondary signals in lithium ferrite. Figure 4 presents oscillograms illustrating the dependence of SPE and TPE signals and their secondary signals on a short repetition period of RF pulses T , compared to the transverse (T_2) and longitudinal (T_1) relaxation times [11].

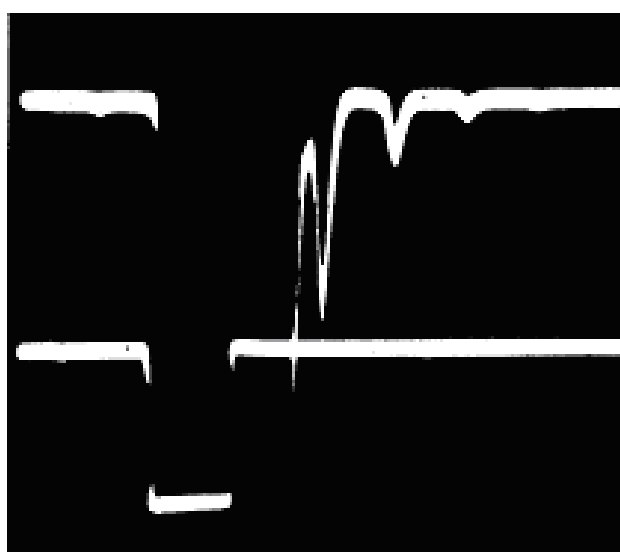


Figure 2: Oscillograms of the SPE and its secondary signals from ^{57}Fe nuclei in lithium ferrite. The lower beam indicates the position and duration of the RF pulses ($T=77\text{K}$, $f_{\text{NMR}} = 71.6 \text{ MHz}$, $\tau = 10 \mu\text{s}$, $T = 300 \mu\text{s}$).

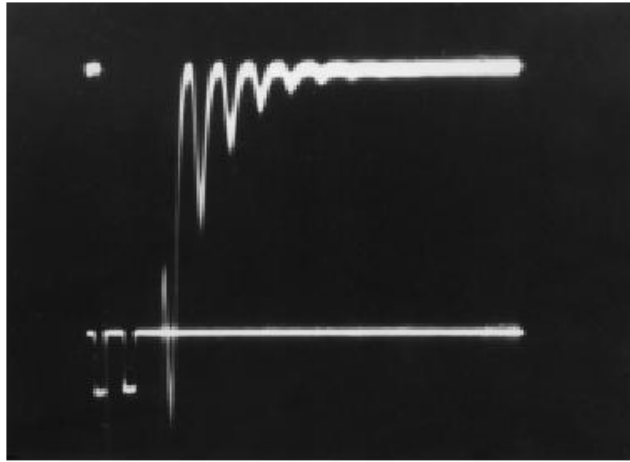


Figure 3: Oscillograms of the SPE and its secondary signals from ^{57}Fe nuclei in lithium ferrite. The lower beam indicates the position and duration of the RF pulses ($T=77\text{K}$, $f_{\text{NMR}}=71.6\text{ MHz}$, $\tau=10\ \mu\text{s}$, $T=300\ \mu\text{s}$).

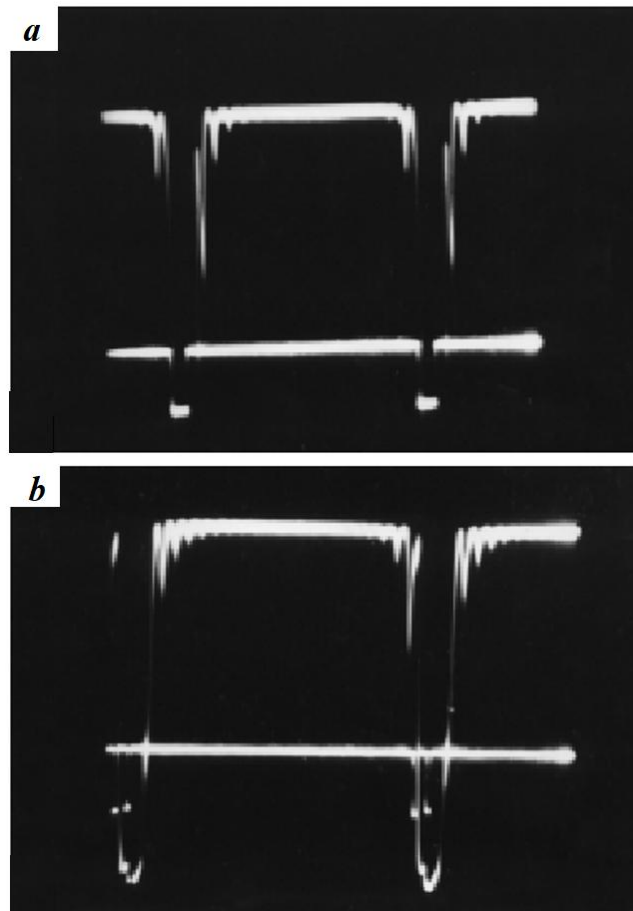


Figure 4: Oscillograms of (a) SPE and (b) TPE signals at a high repetition rate of RF pulses ($T \ll T_1, T_2$, $T=100\ \mu\text{s}$.) in lithium ferrite.

In [19-22] an unusual spin-echo phenomenon a so-called cumulative NMR single-pulse echo effect were reported in lithium ferrite and cobalt, when a train of echoes generated by a repeating single RF pulse sequence exhibits the growth rather than damping.

Similar effect was earlier observed for photon echoes generated by a repeating two light pulse sequence [21] and called as the cumulative two-pulse photon echoes. In this case also a train of echoes, generated by a repeating two-pulse sequence, exhibits a growth rather than damping.

This method was further developed in [22] where it was realized other mode of cumulative long-lived optical echo generation - cumulative stimulated photon echo (CSPE).

These experiments showed the possibility to increase of the maximum intensity with the increase of pairs number on the several orders in respect to the ordinary three pulse stimulated echo signal. This makes it possible to obtain the intensive CSPE signals using packets of small intensity pair pulses what essentially improves the energetics of optical memory operation on the basis of long-lived CSPE effect.

This method could be useful also in NMR and NQR allowing one to improve sensitivity of these techniques due to possibility of obtaining intensive cumulative echo signals using small power RF pulses, in particular, it could be used to improve sensitivity for the sensitivity for the remote detection of explosives using NQR [23].

Figures 5 and 6 show the cumulative stimulated single-pulse echoes (CSPE) in lithium ferrite and cobalt at liquid nitrogen temperature at excitation by a series of six RF pulses with different RF pulse powers.

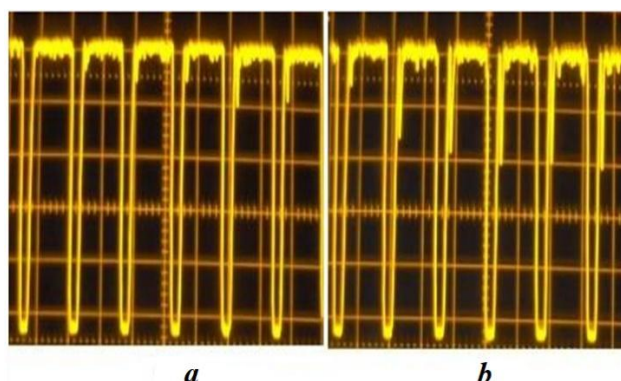


Figure 5: The CSPE in lithium ferrite at $T=77$ K at excitation by six RF pulses with duration $10 \mu\text{s}$ and time intervals between them of $60 \mu\text{s}$. a - RF pulse power is small; b - RF pulse power is optimal [19].

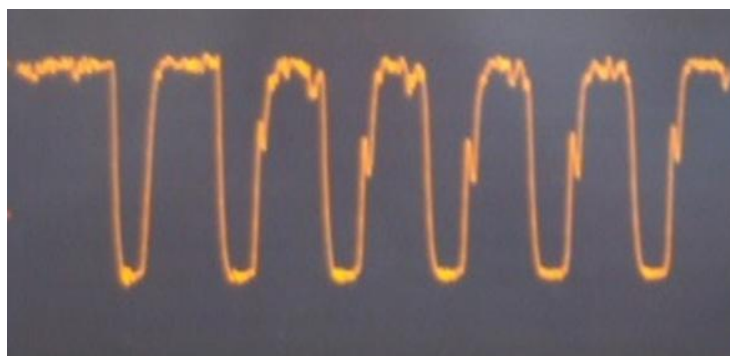


Figure 6: Cumulative echo effect in cobalt during excitation by six $4.5 \mu\text{s}$ duration RF pulses with intervals between them $\tau_1=23 \mu\text{s}$, $f_{\text{NMR}} = 216,8 \text{ MHz}$, $T = 77 \text{ K}$, RF pulse amplitude is $H_1=0.1 \text{ mOe}$ [20]

Figures 7, 8 and 9 illustrate the dependence of SPE and TPE signal intensities, including their secondary components, on the repetition period of RF pulses (T_r) in lithium ferrite and, for comparison, in hexagonal cobalt. The experimental results are consistent with the multiple-pulse and distortion mechanisms of echo formation, which we outline below.

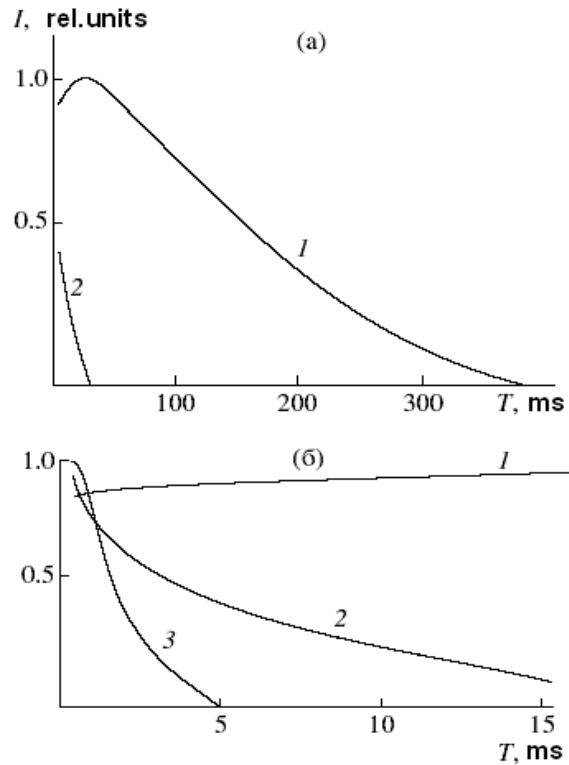


Figure 7: (a) The intensity of (1) the SPE signal and (2) its secondary signal as functions of the repetition period T of RF pulses in lithium ferrite. (b) The initial segment of (1) the SPE signal and (2), (3) its secondary signal as functions of T .

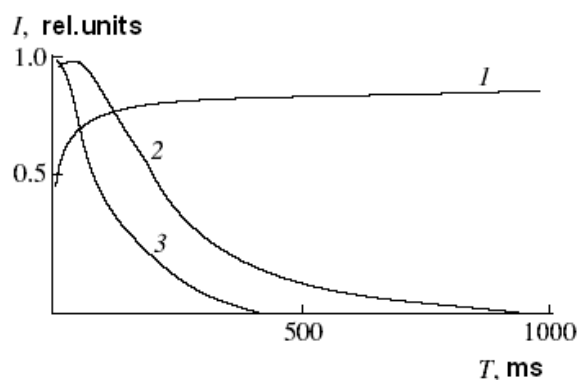


Figure 8: The intensity of (1) TPE signal and (2), (3) its secondary signals as functions of the repetition period T of the RF pulses in lithium ferrite.

For comparison, Figure 9 display the dependences of the SPE and TPE signals on T in cobalt.

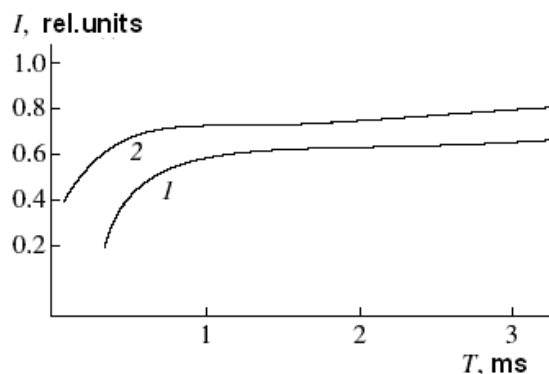


Figure 9: The intensity of (1) SPE and (2) TPE as functions of the period of repetition of the RF pulses T in cobalt.

Shakhmuratova *et al.* [12] used the formalism of statistic tensors to perform a theoretical investigation of the formation of SPE and its secondary signals in the presence of Larmor and Rabi inhomogeneous broadenings of the NMR line, which, e.g., takes place in multidomain ferromagnets when the repetition period of RF pulses T satisfies the following inequality for the characteristic relaxation parameters:

$$T_3 \ll T_2 < T < T_1, \quad (1)$$

Where T_1 and T_2 are the longitudinal and transverse relaxation times, respectively, and T_3 represents inhomogeneous broadening effects.

Under these conditions, the RF cycles are applied to a nonequilibrium spin system, and in the end of each period T we should take into account only the longitudinal component of the nuclear magnetization as the initial condition for the consideration of the dynamics of the spin system [12]. It was shown that the dephasing of the spin-system, which is accumulated in the course of n -fold repetition of the pulsed excitation, is recovered during a time interval following the $(n+1)$ -th “read-out” pulse in the multiple-pulse sequence, which leads to the formation of an SPE and its secondary signals at time moments multiple duration of the RF pulse τ after the termination of the “read-out” pulse.

First, it was shown that the expressions for the components of the nuclear-magnetization vector obtained in [12] by the method of statistical tensors can be obtained directly, following the classical approach, by solving Bloch equations in Hahn’s spin systems. To this end, we use the set of Bloch equations [7, Eqs. (2)] that take into account both type of inhomogeneous broadenings of NMR lines:

$$\dot{X}_j = \Delta\omega_j Y_j - \omega_j Z_j; \quad \dot{Y}_j = \Delta\omega_j X_j; \quad \dot{Z}_j = \omega_j X_j, \quad (2)$$

where $\omega_j = \gamma_n \eta H_1$ is the pulse amplitude in frequency units, γ_n is the nuclear gyromagnetic ratio, η is the coefficient of enhancement of the RF field, and

$$X_j = m_{xj} / m; \quad Y_j = m_{yj} / m; \quad Z_j = m_{zj} / m; \quad \Delta\omega_j = \omega_{\text{NMR}} - \omega_{\text{RF}}, \quad (3)$$

Where m is an equilibrium value of nuclear magnetization.

The solution to the set of equations (1) under equilibrium initial conditions $X_j(0) = Y_j(0) = 0$ and $Z_j(0) = 1$ has the form:

$$\begin{aligned}
 X_j &= -\sin\theta_j \sin\Delta\omega_j t; \\
 Y_j &= -\sin\theta_j \cos\theta_j \cos\Delta\omega_j t + \sin\theta_j \cos\theta_j; \\
 Z_j &= \sin^2\theta_j \cos\Delta\omega_j t + \cos^2\theta_j,
 \end{aligned} \tag{4}$$

where θ_j is the angle between $\mathbf{H}_{\text{eff}} = \frac{1}{\gamma_n} (\Delta\omega_j \hat{z} + \omega_1 \hat{y})$ (\hat{z} and \hat{y} are the unit vectors of the rotating coordinate system) and Z axis:

$$\sin\theta_j = \frac{\omega_1}{\Delta\omega'_j}; \quad \cos\theta_j = \frac{\Delta\omega_j}{\Delta\omega'_j},$$

and $\Delta\omega'_j = \sqrt{\Delta\omega_j^2 + \omega_1^2}$ is the angular velocity of the precession of the j -th isochromate about \mathbf{H}_{eff} .

After the pulse is switched off, the motion of m_j is described by Eq. (2) and represents the precession about the Z axis with a frequency $\Delta\omega_j$. The expressions for the components of the magnetization take on the following form:

$$\begin{aligned}
 X_j &= -\sin\theta_j \sin\Delta\omega'_j \tau \cos\Delta\omega_j t + \sin\theta_j \cos\theta_j (1 - \cos\Delta\omega'_j \tau) \sin\Delta\omega_j t; \\
 Y_j &= \sin\theta_j \sin\Delta\omega'_j \tau \sin\Delta\omega_j t + \sin\theta_j \cos\theta_j (1 - \cos\Delta\omega'_j \tau) \cos\Delta\omega_j t \\
 Z_j &= \sin^2\theta_j \cos\Delta\omega'_j \tau + \cos^2\theta_j.
 \end{aligned}$$

It can easily be shown that the solution to Eq. (2) under the equilibrium initial conditions and fulfillment of condition (1) after the action of a series of n "preparatory" pulses and the termination of the "read-out" ($n+1$)-th pulse has the form

$$\begin{aligned}
 X_j &= (\sin^2\theta_j \cos\Delta\omega'_j \tau + \cos^2\theta_j)^n \cdot \\
 &[-\sin\theta_j \cos\Delta\omega'_j \tau \cos\Delta\omega_j t + \sin\theta_j \cos\theta_j (1 - \cos\Delta\omega'_j \tau) \sin\Delta\omega_j t] \\
 Y_j &= (\sin^2\theta_j \cos\Delta\omega'_j \tau + \cos^2\theta_j)^n \cdot \\
 &[\sin\theta_j \sin\Delta\omega'_j \tau \sin\Delta\omega_j t + \sin\theta_j \cos\theta_j (1 - \cos\Delta\omega'_j \tau) \cos\Delta\omega_j t]
 \end{aligned}$$

where the designations borrowed from [12] were used: $x = \Delta\omega_j / \omega_1$, $a = \frac{\eta}{\eta}$ ($a = \omega_1 / \omega_1$), $y = \omega_1 \Delta t$ is the average value of the pulse area; Δt is the pulse duration, and $b = \omega \tau$ is the current time after termination of the pulse.

Correspondingly, the expressions for the transverse magnetizations take on the form:

$$\begin{aligned}
 X_j &= \left(1 - \frac{a^2}{a^2 + x^2} \left[1 - \cos y \sqrt{a^2 + x^2} \right] \right)^n \cdot \\
 &\left[\cos bx \frac{ax}{a^2 + x^2} \left(1 - \cos y \sqrt{a^2 + x^2} \right) + \sin bx \frac{a}{\sqrt{a^2 + x^2}} \sin y \sqrt{a^2 + x^2} \right]
 \end{aligned}$$

$$Y_j = \left(1 - \frac{a^2}{a^2 + x^2} \left[1 - \cos y \sqrt{a^2 + x^2} \right] \right)^n \cdot \left[\sin bx \frac{ax}{a^2 + x^2} \left(1 - \cos y \sqrt{a^2 + x^2} \right) + \cos bx \frac{a}{\sqrt{a^2 + x^2}} \sin y \sqrt{a^2 + x^2} \right], \quad (6)$$

which is equivalent to Eqs. (14) in [12].

The factor in the n-th power has the simple physical meaning of the longitudinal nuclear magnetization after the action of n “preparatory” pulses and reflects the memory of the spin system for its excitation by the pulse sequence.

The expressions for the transverse components of the nuclear magnetization (6) coincide with the corresponding expressions obtained in [12] by the method of statistical tensors.

The single-pulse excitation for the case of a non-resonant excitation was considered in [6] (where a simple analytical expression for the amplitude of the SPE was obtained) and for the case of a resonance excitation, in [12]. It was shown in [12] that upon single-pulse action in the presence of a double frequency inhomogeneity at the trailing edge of the oscillatory free-induction decay (OFID) signal, a step-like anomaly is formed, which rapidly evolves into the primary echo signals arising after a multiple-pulse excitation. It was also established in [12] that the primary SPE falls off more slowly with increasing T than the secondary signals, which is not responds to the irreversible loss of the phase memory of the system when nT begins significantly exceed T₁.

A theoretical analysis using expressions obtained for the nuclear magnetization in [12] in the presence of both Larmor and Rabi inhomogeneous broadenings of the NMR line showed the existence of an SPE along with its weaker secondary signals that are formed upon the multipulse excitation under condition (1). These signals arise as a result of a complex superposition of oscillatory free-induction decay signals that propagate outside the duration of a single RF pulse owing to the successive accumulation of dephasing within each pulse of the sequence. The effect is also present in the case of systems that have only a large Larmor broadening, but it manifests itself much more strongly upon the simultaneous existence of both frequency nonuniformities, which is characteristic of, e.g., multidomain ferromagnets. The theoretical results were confirmed experimentally on the example of ferromagnets such as Fe and VFe.

SPE signals and its secondary signals, as well as the effect of their enhancement with increasing frequency of repetition of RF pulses $f_p=1/T$ were revealed. In addition, a faster disappearance of the secondary echo signals as compared to the SPE signal was found with decreasing f_p . However, the experimental conditions did not make it possible to study the dependences of their amplitudes on the repetition period T. This was done in [11] owing to the large intensity of the signals observed in lithium ferrite. In addition, in this work secondary signals of the TPE (Figure 7) were studied. The presence of a large number of secondary echo signals is seen. It is also seen that the dependence of the amplitudes of the SPE and its secondary signals on T is similar to the corresponding dependences of the secondary TPE signals (Figure 8, curves 2 and 3), which indicates the common nature of the mechanisms of their formation. Earlier, analogous phenomena for simpler systems, such as protons in aqueous solutions of paramagnetic ions and aluminates, were studied in [1,24].

As is known, in such systems both phenomenological and quantum theories of spin echo [1,25] predict the formation of only a single echo signals upon the action of a series of two RF pulses on the spin system.

In [1], the possibility of the appearance of additional echo signals was predicted for the case where the action of RF pulses is preceded by a nonequilibrium of the spin system, and this effect was interpreted theoretically and compared with the experiment. In the case under consideration, the presence of a large number of secondary echo signals cannot also be explained by quadrupole effects [13] or by the presence of a dynamic frequency shift, since the isotope ^{57}Fe has a zero quadrupole moment and no DFS effects have been found in lithium ferrite at liquid-nitrogen temperatures. Note also that when the distortion mechanism is effective, the TPE and SPE signals change in a similar way upon the change in the conditions of their excitation [11]. However, their dependences on T shown in Figure 9 are quite different.

In addition, in this case, the following relationship between the transverse relaxation times of TPE (T_2) and SPE (sT_2) is usually observed: $^sT_2 = (0.5-0.8) T_2$ [11]. As to lithium ferrite, these relaxation times differ by more than an order of magnitude; e.g., at $f_{\text{NMR}}=73.2$ MHz, they are $T_2=1200 \mu\text{s}$ and $^sT_2 = 40 \mu\text{s}$. The oscillograms shown in Figure 4 are analogous to those obtained in [26] for protons in aqueous solutions in the case of short repetition periods of the RF pulses $T \ll T_1, T_2$.

Further, it was established, using a storage oscilloscope, that the SPE disappears as the repetition period of RF pulses T increases to above $T = 500 \mu\text{s}$ and that the secondary signals disappear even earlier. This indicates that the principal mechanism of echo formation in lithium ferrite under given experimental conditions is the multiple-pulse mechanism. Indeed, it is seen from Figure 8 that at large repetition periods ($T \gg T_1$) the SPE signals in cobalt do not disappear but remain constant in magnitude in accordance with the edge mechanism of the SPE formation in these materials [11].

In work [11] it was shown that SPE properties in lithium ferrite could be understood in frames of multiple-pulse non-resonant mechanism allowing for the nonequilibrium of spin-system before each RF pulse of RF pulse train.

In work [27] it was established that the single-pulse echo in cobalt was formed by the distortion mechanism of the exciting radio-frequency pulse edges due to mainly hyperfine field anisotropy beginning with a certain value of radio-frequency pulse power. Before this threshold radio-frequency power the single-pulse is formed by non-resonant mechanism as in lithium ferrite.

For this aim a comparative study of SPE in lithium ferrite and cobalt was made to clear out the SPE echo formation in cobalt possessing a highly anisotropic HF. The SPE in cobalt was firstly observed by Stearns [3] contrary to the theoretical estimates indicating its absence. Particular intensive SPE signals were observed in the HCP phase, characterized by a strong anisotropy of the HF. In subsequent works [9,16] to explain the observed SPE effect it was proposed the distortion mechanism of SPE formation responsible to the RF fronts distortions arising due to the transient processes in the radio engineering circuits at turning on and out the RF pulse. In this case, the edges of RF pulse play a role of two RF pulses in the Hahn TPE method and the emergence of SPE could be explained in accordance with the experiment [9,16].

In [27] an alternative internal mechanism for the RF pulse fronts distortion associated with the role of strong HF anisotropy in cobalt was proposed. At the deviation of electron magnetization when turning on and out a RF pulse it appears the significant distortions of oscillating local HF field acting on nuclei at response of electron magnetization to RF pulse excitation due to the HF anisotropy.

The role of strong HF anisotropy in cobalt has already been clearly demonstrated in the TPE and SPE decay envelope modulation under the influence of a weak LF magnetic field in cobalt [10]. Accordingly [27] the SPE in cobalt is formed by the distortion mechanism due to mainly the HF anisotropy starting from a certain threshold value of RF power. Below this threshold value SPE is formed by the multiple-pulse non-resonant mechanism as in lithium ferrite where the distortion mechanism is ineffective due to a weak HF anisotropy.

As known in the case of single-pulse excitation the presence of resonance in lithium ferrite could be revealed by two-pulse stimulated echo method (TPSE) [27] at excitation by a pair of identical RF-pulses. The TPSE signal is formed in time moment τ (τ is the first RF pulse duration) after the trailing edge of the second RF pulse (Figure 10).

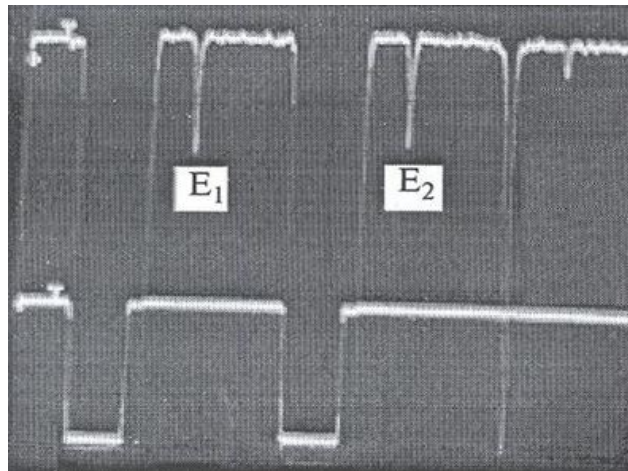


Figure 10: SPE (E_1) and TPSE (E_2) in lithium ferrite upon action of two RF pulses of equal length t_p , $f_{NMR}=71$ MHz, $\tau_1 = \tau_2 = 8$ μ s, $\tau_{12}=22$ μ s.

In Figure 11 it is presented the SPE and TPSE dependences on the repetition frequency of pair RF pulse train in lithium ferrite.

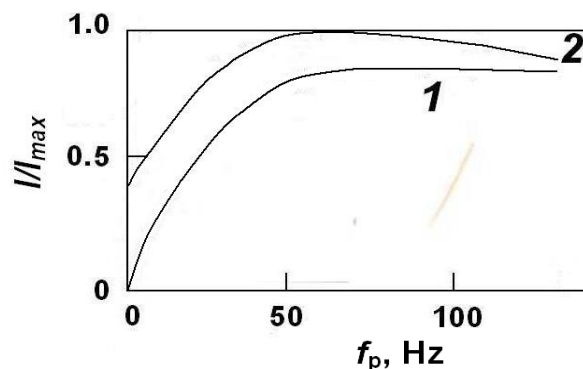


Figure 11: SPE (curve 1) and TPSE (curve 2) dependences on the repetition frequency of RF pulses in lithium ferrite at: $\tau_1 = \tau_2 = 9$ MHz, $\tau_{12}=22$ μ s, $f_{NMR}=70.5$ MHz, H_1 is optimal.

It is seen that in the case of single pair excitation the TPSE response is not absent, as in case of SPE [23]. In [28] the TPSE properties in cobalt were studied. It was revealed that both non-resonant and distortion mechanisms make contributions in the spin-echo relaxation processes of TPSE. In case of cobalt the SPE signal was always present since some RF pulses power due to the effectiveness of distortion mechanism of SPE formation in Co.

As comparison, in lithium ferrite the SPE signal is absent at a single excitation limit. At repetition frequency different from zero it appears also additional a multiple-pulse contribution in the SPE also.

Figure 5 shows the cumulative SPE effect in lithium ferrite observed at excitation by a series of six RF pulses, each of them with duration 3 μ s.

In [27] the optimal conditions for observation of contributions of both mechanisms to the intensity of SPE and TPSE depending on the value of hyperfine field anisotropy was defined.

In Fig. 12 the dependences of investigated echo responses on RF pulse power are shown for three values of NMR frequency in the part of spectrum where the anisotropic contribution to the HF field strongly increases with frequency, as it was established using the magnetic-video pulse excitation technique [27].

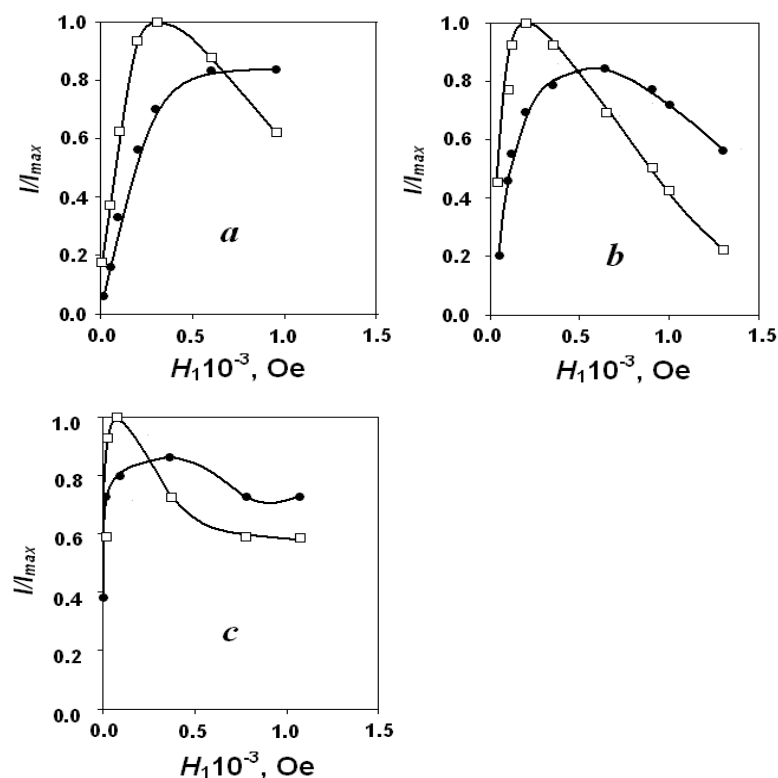


Figure 12: SPE and TPSE dependences on the RF magnetic field amplitude H_1 at three different NMR frequencies in cobalt at $\tau_1 = \tau_2 = 10$ MHz, $\tau_{12} = 40$ μ s, (a) $f_{\text{NMR}} = 217$ MHz; (b) $f_{\text{NMR}} = 218.6$ MHz; (c) $f_{\text{NMR}} = 219.6$ MHz, [27]

As is seen from Figure 12, the SPE in cobalt has an optimal value at much greater magnitude of RF power than the TPSE signal which includes the multiple-pulse non-resonant contribution along with the distortion one.

Besides, it is seen from Figure 10 (a, b, c) that, at the increase of HF anisotropy, the optimal value of RF power for observation of SPE, which is formed mainly by the distortion mechanism, is reduced, which counts in favor of our assumption on the definite role of HF anisotropy in SPE formation in cobalt at $T \gg T_1$

In Figure 13 SPE and TPSE dependences on the repetition frequency of the RF pulse pair at three increasing values of RF powers from low to high values and an intermediate one is shown.

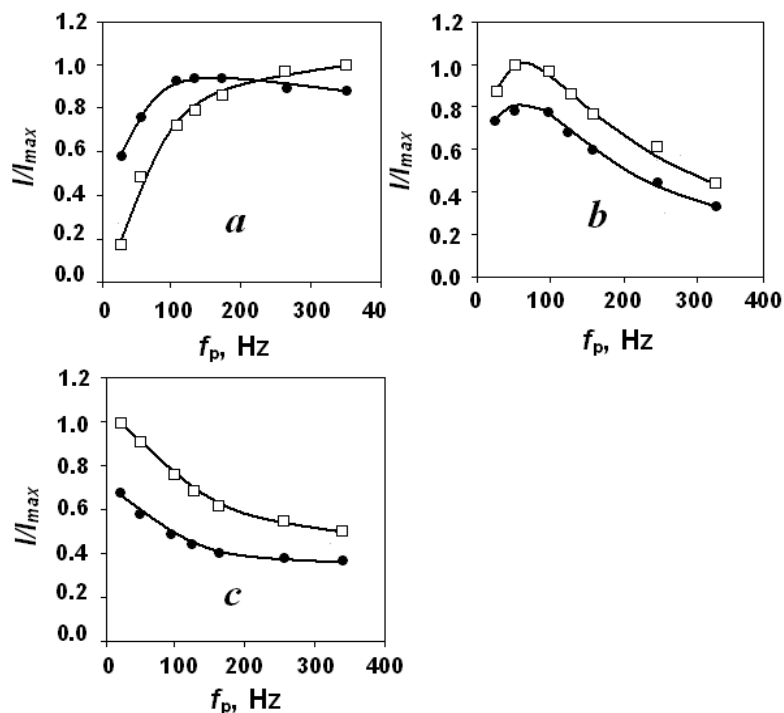


Figure 13: SPE and TPSE dependences on RF pulse repetition frequency f_p in pure cobalt at three different RF pulse power, (a) H_1 min $\sim 0.1 \cdot 10^{-3}$ Oe; (b) H_1 middle $\sim 0.5 \cdot 10^{-3}$ Oe; (c) H_1 max $\sim 1.2 \cdot 10^{-3}$ Oe, [23].

As is seen from the figures, images the multiple-pulse contribution is the main one in the case of low-power RF. This fact is comparing with a similar dependence in the case of lithium ferrite. Then, upon an increase in the RF power, the contribution of the distortion mechanism increases, and, at the maximum power, the dependence becomes like the one observed in cobalt where the distortion mechanism is the main one [11]. In Figure 13 a, b, and c we show dependences for three different increasing RF pulse powers confirming this supposition.

The fact that, before some threshold value of RF pulse power, the multiple-pulse mechanism is main in cobalt is also illustrated by oscillograms shown in Fig. 14 presenting the cumulative echo features observed also in lithium ferrite (cumulative echo effect) in Figure 5, i.e. cumulative echo enhancement at the response of three pulse excitation at low RF pulse powers.

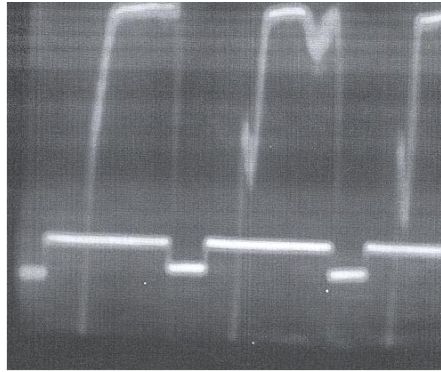


Figure 14: Cumulative single-pulse echo effect in cobalt [11].

The study of the dependence of the intensity of an SPE on the power of RF pulses in cobalt showed that at low powers of RF pulses, only a free precession signal is observed [27] at a single-pulse excitation mode. Besides it, signals of a cumulative echo [27], Figure 14, are also observed in this case, as in the case of the multiple-pulse mechanism of SPE formation [11]. The SPE signal in cobalt, formed by the distortion mechanism, occurs at a sufficiently high power of the RF pulse [27].

To implement a single-pulse analog of the SPE signal in the SPE method, the spin system was excited by a more complex RF pulse, during which the direction of H_{eff} changes sufficiently quickly at the action of a pair of MVP pulses under the condition $\Delta\omega'_j\tau_m \ll 1$, where $\Delta\omega'_j = (\Delta\omega_j^2 + \omega_j^2)^{1/2}$ and τ_m - the duration of the MVP [29]. In our case, a sharp change in the direction of H_{eff} within the RF pulse is achieved when the pair of MVP pulses turn on near the trailing edge of a sufficiently long RF pulse. In this case, only one so-called magnetic echo (ME) signal is observed, and other signals, which are formed by the combined action of the leading edge of the RF pulse and MVP pulses, do not interfere with it, Figure 15.

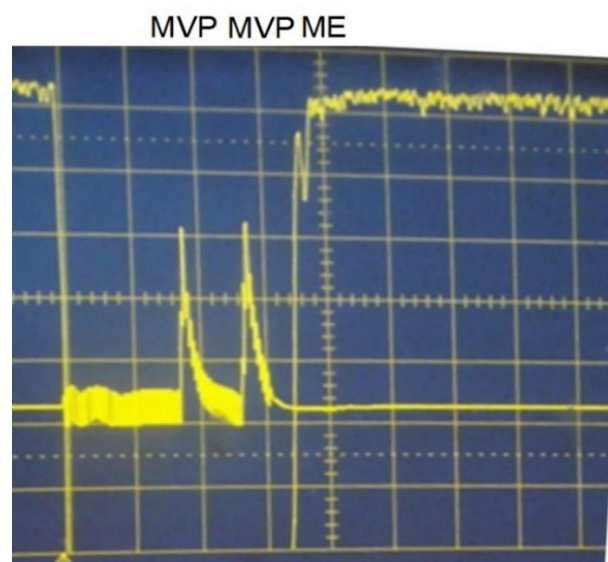


Figure 15: Oscillogram of a single excitation by an RF pulse combined with two MVPs, generating a ME signal at the frequency of $\nu = 213$ MHz, with an RF pulse duration of $\tau_{\text{RF}} = 60$ μs , MVP durations $\tau_m = 1$ μs , $T = 293$ K. The lower trace is a wave-meter signal showing the location of MVP pulses within the RF pulse.

Rapid changes in the direction of H_{eff} in the RCS occur when a DW is displaced under the action of MVP pulses due to the anisotropy of the HFF and the inhomogeneity of the factor η in the DW.

Next, we study the properties of this analog of the SPE signal, for brevity called the magnetic echo (ME) signal, formed under the combined action of RF and a pair of MVP pulses, Figure 16.

Previously, in [30], the effect of the formation of an edge magnetic echo (EME) signal was studied under the combined action of an MVP and the trailing edge of a sufficiently long RF pulse.

In this work, it was shown that the EME signal, an analog of the SPE signal that occurs in this case, is formed by the mechanism of distortion of the fronts of an effective RF pulse, which is formed jointly by an MVP pulse and the trailing edge of a sufficiently long RF pulse above a certain MVP threshold amplitude associated with the DW pinning force when the power of the RF pulse was sufficient to observe the normal SPE signal.

The impact of two MVP pulses makes it possible to control the degree of influence of the mechanism of distortion of both fronts of the effective RF pulse depending on the amplitude of the MVP. Figure 16 shows the dependence of the ME intensity on the amplitude of the MVP pulses.

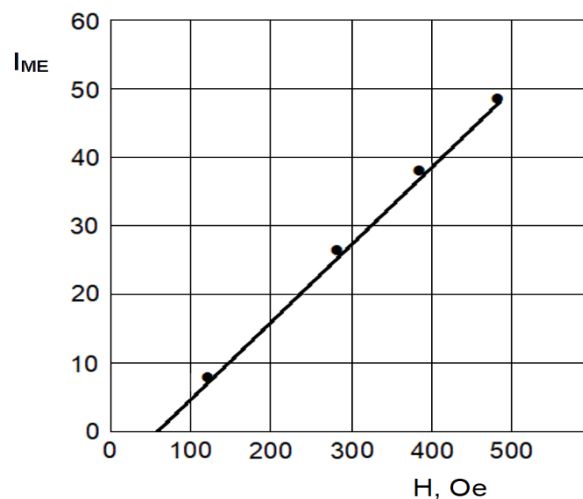


Figure 16: Dependence of the intensity I_{ME} of the magnetic echo (ME) on the amplitudes of the two similar magnetic video-pulses (MVPs).

When the MVP amplitudes exceed H_0 for the ME observation, the ME signal is formed by the distortion mechanism and is observed under a single combined action of RF and a pair of MVPs.

At the MVP amplitudes $H < H_0$, the ME signal is formed by a multiple-pulse mechanism and is not observed at the application of a single combined RF and the pair of MVPs excitation, but only at repeated exposure to RF and a pair of MVPs with f_r frequency, Figure 17a.

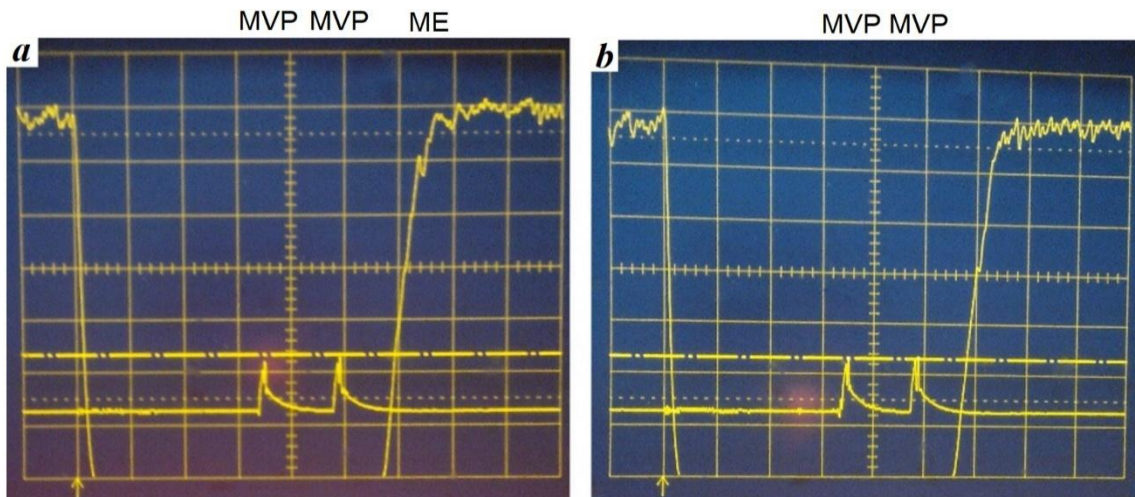


Figure 17: Oscillogram of ME signal excitation by an RF pulse combined with two MVPs, at the NMR frequency $\nu = 213$ MHz, with RF pulse duration $\tau_{RF} = 60$ μ s, MVP pulse durations $\tau_m = 1$ μ s, MVP amplitude $H = 30$ Oe, $T = 293$ K: a) multiple excitations with a repetition frequency of RF and a pair of MVPs action $f_r = 100$ Hz; b) single excitation with RF and a pair of MVPs. The lower trace is a signal from wave-meter showing the position of the MVPs within the RF pulse.

Next, we present the results of a comparative study of the transverse relaxation processes T_2 of ordinary TPE and SPE signals with the transverse relaxation of the ME signal, Figure 18.

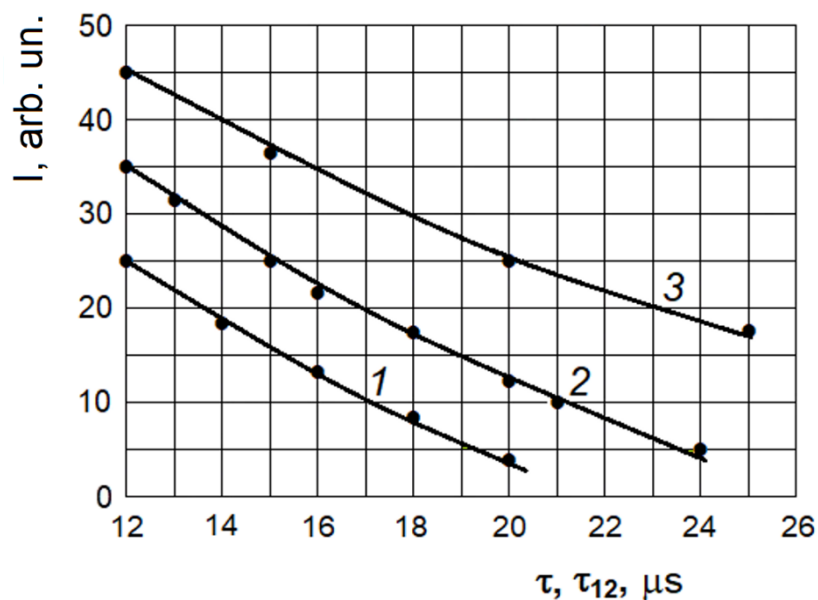


Figure 18: The intensities I of decay envelopes of ME (1), SPE (2) and TPE (3) signals depend on the duration of the effective RF pulse (curve 1) and RF pulse (curve 2) τ , as well as the distance between RF pulses τ_{12} (curve 3), respectively.

Figure 16 shows the amplitude dependence of the ME on the interval between two MVP pulses τ , as well as the amplitude dependences of the SPE and TPE depending on the

duration of the RF pulse τ and the interval τ_{12} between two TPE exciting RF pulses, respectively.

As can be seen from Figure 8, the SPE and ME signals are characterized by practically similar transverse relaxation times $T_2^{\text{ME}} = T_2^{\text{SPE}} = 30 \mu\text{s}$, which are somewhat shorter as compared to T_2 for TPE, in accordance with [16,29].

Based on the obtained experimental results, it can be assumed that the ME signal is formed by the mechanism of distortion of the fronts of the effective RF pulse, formed by a pair of MVP pulses in combination with the RF pulse, when the amplitudes of the MVP pulses exceed the threshold value of the pinning force H_0 , measured by the effect of these MVP pulses on the intensity of the TPE as in [30]. It should be noted that as the amplitude of one of the MVPs decreases below H_0 , the ME signal disappears. Thus, the leading role is played by the distortion of the fronts of the effective RF pulse under the action of a pair of MVP pulses, which is caused by the sufficiently fast displacements of the DWs, due to the anisotropy of the HFF and the inhomogeneity of the RF field amplification factor η .

The experimental dependences of the ME signal can be qualitatively understood within the framework of a simple model similar to that used in [30]. Let us assume that under the combined action of RF and a first MVP pulse, a DW reversibly shifts at a distance Δx proportional to the MVP amplitude: $\Delta x \sim v\tau_d = S(H - H_0)\tau_m$, when the MVP amplitude H exceeds the DW pinning force H_0 .

Under the combined action of RF and MVP, the magnitude and direction of the effective magnetic field H_{eff} at the nuclei of the Δx layer in the RSC changes abruptly due to the corresponding changes in the HFF and the factor η . According to the non-resonant model of the formation of the SPE [31], the impact of the first MVP is equivalent to the effect of the leading edge of the RF pulse during the formation of the SPE. In this case, the role of the second front of the RF pulse, rephasing the transverse magnetization arising as a result of the action of the first MVP, is played by the second MVP. In this case, the ME amplitude will be proportional to the number of nuclei in the layer Δx formed when the DW is displaced by the first MVP: $I_{\text{ME}} \sim \Delta x/L$, where L - the width of the excited section of the DW under the influence of an RF pulse, while the jump-like change in the NMR frequency in the RCS $\Delta\omega'_j = (\Delta\omega_j^2 + \omega_1^2)^{1/2}$ must satisfy the condition $\Delta\omega'_j \cdot \tau_m \ll 1$ at which the precession period $T' = 2\pi/\Delta\omega'_j$ of nuclei in RSC must be larger than MVP duration τ_m : $T' \gg \tau_m$.

As is known, the NMR spin echo phenomenon can be used to store and manipulate large amounts of information [32-35]. Examples are functional electronic devices, spin processors, and the development of quantum computers. Spin processors based on NMR spin echo can also be used for analog processing of RF pulses in order to increase the processing speed of wideband signals in real time, which is difficult to achieve using traditional digital process engineering methods [36]. An echo processor using the NMR spin-echo phenomenon in magnetic materials can play the role of such an analog processor. The importance of using a magnetic material is that no external magnetic field is required, and there is significant amplification of the spin echo signal from the RF amplification effect in magnetic materials. The SPE method can provide practically the same information about the spin system as the two-pulse echo method. The properties of SPE and the conditions for its observation must be known to account for spin processor's operation based on NMR single-pulse echo phenomenon. In addition, with sufficient signal strength, it is possible to develop a device

for processing RF pulses based on the phenomenon of SPE. The advantage of such a system is that it is not necessary to read the pulses in an RF sequence and that the complexities associated with the need to synchronize the write and read pulses are eliminated.

CONCLUSION

Fundamental mechanisms of single-pulse echo formation in magnets was investigated on example of lithium ferrite and cobalt. Properties of a single-pulse echo and its secondary signals, as well as of secondary signals of a two-pulse echo of ^{57}Fe nuclei in lithium ferrite are studied comparatively with ones in cobalt. The experimental results obtained indicate the efficiency of the multiple-pulse mechanism of the single-pulse echo and its secondary signals formation in lithium ferrite, as well as in cobalt at low powers of radio-frequency pulses. At radio-frequency powers above some threshold value the single-pulse echo in cobalt is formed by the distortion mechanism of a radio-frequency pulse.

It was established that SPE in cobalt is formed by two mechanisms: multiple-pulse and distortion ones depending on the RF pulse power. At low powers the SPE in cobalt is formed by multiple-pulse mechanism as SPE in lithium ferrite. At a higher RF pulse power the distortion mechanism is more effective. The optimal value of RF pulse power for distortion mechanism depends on the value of hyperfine field anisotropy. This experimental observation makes it possible to conclude that the distortion of RF pulse fronts, which are necessary for the SPE formation in frames of distortion mechanism, are caused by mainly a strong hyperfine field anisotropy in cobalt.

A comparative study of the formation mechanisms of a single-pulse echo and a magnetic echo formed upon joint excitation by an RF pulse and a pair of magnetic video-pulses has been carried out also. The magnetic echo is an analog of the single-pulse echo signal generated by the mechanism of distortion of the effective RF pulse edges during the domain wall displacement when the amplitudes of magnetic video-pulses exceed the domain wall pinning force. The obtained results testify in favor of the assumption that the single-pulse echo signal in cobalt is formed due to the mechanism of distortion of the fronts of RF pulses due to the displacements of domain walls leading to distortion of the local field on the nuclei due to the anisotropy of the hyperfine field and the inhomogeneity of the gain factor η in the domain walls for sufficiently large RF pulse powers causing the displacements of domain walls. A potential application of NMR spin-phenomenon for operation of spin-echo processors was also discussed.

REFERENCES

1. Bloom, A.L., Nuclear Induction in Inhomogeneous Fields, *Phys.Rev.*1955, vol. 98, no.4, pp.1105-1111.
2. Hahn E.L., Spin Echoes, *Phys. Rev.* 1950., vol. 80, no.4, pp.580-594.
3. Stearns, B.M., Origin of Single-Pulse Echo in Co, *AIP Conf. Proc.*, 1973, vol. 2, no.10, pp.1644-1647.
4. Schenzle, A., Wong, N.C. and Brewer, R.G., Oscillatory Free-Induction Decay, *Phys. Rev.A*, 1980, vol.21, no.3, pp.887-895.

5. Kunimoto, M, Endo, T., Nakanishi, S. and Hashi, T., Oscillatory Free-Induction Decay and Oscillatory Spin Echoes. *Phys. Rev: A*, 1982, vol. 25, pp.2235-2246.
6. Bun'kov, Yu.M., Dumesh, B.S. and Kurkin, M.I., Single-Pulse Echo in Systems with a Dynamic Frequency Shift, *Pis'ma Zh. Eksp. Teor. Fiz.*, 1974, vol. 19, no. 4, pp.216-219.
7. Chekmarev, V.P., Kurkin, M.I. and Goloshchapov, S.I., Mechanism of Formation of Single-Pulse Echo in Hahn's Spin Systems, *Zh. Eksp. Teor. Fiz.*, 1979, vol. 76, no. 5, pp. 1675-1684.
8. Smolyakov, B.P. and Khaimovich, U.P., Signals of Polarized Echo and Induction Excited by Pulses of Various Duration, *Zh. Eksp. Teor. Fiz.*, 1979, vol. 76, no. 4, pp. 1303-1308.
9. Tsifrinovich, V.I., Mushailov, E.S., Baksheev, N.V., *et al.*, Nuclear Single-Pulse Echo in Ferromagnets, *Zh. Eksp. Teor. Fiz.*, 1985, vol.88, no.4, pp.1481-1489.
10. Akhalkatsi, A.M., Mamniashvili, G.I., On the Role of Pulse Edges in the Single-Pulse Spin-Echo Technique, *Phys. Met.Metallogr.*, 1996, vol. 81, no. 6, pp.632-635.
11. Akhalkatsi, A.M., Mamniashvili, G.I., Gegechkori, T.O., Ben-Ezra, S., On the mechanism of formation of a single-pulse echo of ⁵⁷Fe nuclei in lithium ferrite, *Phys. Met. Metallogr.* 2002, vol. 94, no. 1, pp. 33-39.
12. Shakhmuratova, L.N. Fowler, D.K. and Chaplin, D.H., Fundamental Mechanisms of Single-Pulse NMR Echo Formation, *Phys. Rev. A*, 1997, vol. 55, no. 4, pp. 2955-2967.
13. Kurkin, M.I. and Serikov, V.V., On the Nature of Secondary Spin Echoes in the MnBi Alloy, *Fiz. Tverd. Tela* (Leningrad), 1974, vol. 16, no. 4, pp. 1177-1186.
14. Kurkin, M.I. and Turov, E.A., *NMR in Magnetically Ordered Materials and its Application*, Moscow: Nauka, 1990.
15. Kunevich, A.V. and Pavlov, G.D., Magnetic Materials for Devices of the Functional Electronics, *Electron. Tekh.: Ser. Mater.*, 1985, no.6 (1135), pp.1-68.
16. Kiliptari, I.G. and Tsifrinovich, V.I., Single-Pulse Nuclear Spin Echo in Magnets, *Phys. Rev. B: Condens. Matter*, 1998, vol. 57, no. 18, pp. 11554-11564.
17. Gavasheli, T.A., Mamniashvili, G.I., Shermadini, Z.G., Zedginidze, T.I., Petriashvili, T.G., Gegechkori, T.O., Janjalia, M.V. *J. Magn. Magn. Mater.*, 2020, vol. 500, pp. 166310.
18. Fokina, N.P. and Khutsishvili, K.O., Nuclear Spin Echo Enhancement in Magnets Caused by Resonator Effects, *Fiz. Met. Metalloved.*, 1990, no. 8, pp. 65-72.
19. Gavasheli, T.A., Mamniashvili, G.I., Gegechkori, T.O., Shermadini, Z.G., Ghvedashvili, G., Cumulative stimulated echo in magnets, XXI st International Seminar/Workshop "Direct and Inverse Problems of Electromagnet and Acoustic Wave Theory (DIPED), 2016 Sep 26 (pp. 123-126). IEEE.
20. G.I.Mamniashvili, T.O.Gegechkori and Z.G.Shermadini. "Cumulative single-pulse NMR echoes in cobalt", *Appl. Phys. Res.* Vol. 7, N6, pp. 26-33 (2015).
21. A.Schenzle, R.G.DeVoe, R.G.Brewer "Cumulative two-pulse photon echoes. *Phys Rev A* 30, pp. 1866-1872 (1984).
22. V.A. Zuikov, D.F.Gaĭnulin, V.V.Samartsev, M.F.Stel'makh, M.A.Yufin and M.A.Yakshin. "Accumulated long-lived optical echo and optical memory", *Soviet Journal of Quantum Electronics*, Vol. 21, N4, pp. 477 (1991).
23. W.Prescott, J.B.Miller, C.Tourigny, K.I.Sauer. " Nuclear quadrupole resonance single-pulse echoes", *J. Magn. Res.* Vol. 194, pp. 1-7 (2008). <http://dx.doi.org/10.1016/j.jmr.2008.05.020>

24. Alekseev, B.F. and Gadaev, V.D., Secondary Proton Echoes upon Periodic Two-Pulse Excitation, *Pis'ma Zh. Eksp. Teor. Fiz.*, 1975, vol.22, no.7, pp.357-360.
25. Das, T.P., Saha, A.K. and Roy, D.K. Quantum-Mechanical Analysis of Spin-Echo Phenomena, *Proc. Roy. Soc. (London)*, 1955, vol. 227, no. 1170, pp. 407-421.
26. Pfeifer, H., Dolega, V. and Winkler, H., Ober Weitere Echoes bei der Hahnschen Spinechomethode, *Ann. Phys.*, 1955, vol. 15. no. 3-4, pp. 246-248.
27. Mamniashvili, G.I., Gegechkori, T.O., Akhalkatsi, A.M., Gavasheli, T.A., On the role of the hyperfine field anisotropy in the formation of a single-pulse NMR spin echo in cobalt, *J. Supercond. Nov. Magn.*, 2015, vol. 28, no. 3, pp. 911-916.
28. Zviadadze, M.D., Mamniashvili, G.I., Gegechkori, T.O., Akhalkatsi, A.M., Gavasheli, T.A., Two pulse stimulated echo in magnets, *Phys. Met. Metallogr.*, 2012, vol. 113, no. 9, pp. 849-854.
29. Mamniashvili, G., Gegechkori, T., Janjalia, B.M., Gogishvili, P., Investigation of the single-pulse NMR echo origin in cobalt using additional magnetic video-pulses, *Magn. Reson. Solids*, 2022, vol. 24, no. 1, 22102
30. Mamniashvili, G.I., Gegechkori, T.O., Analogue of a single-pulse echo signal in cobalt, formed under the action of an additional magnetic video pulse, *J. Appl. Spectrosc.*, 2021, vol. 88, no. 5, pp. 965-569.
31. Chekmarev, V.P., Mamniashvili, G.I., Multipulse excitation analog in the single-pulse echo method, *Fiz. Met. Metallov*. 1981, vol. 51, 685-689.
32. Petrov, M., Smolensky, G., Stepanov, S., Petrov, A., Information processing by a nuclear spin echo in magnetically ordered crystals, *IEEE Trans. Magn.* 1977, vol. 13, no. 1, 934-935.
33. Nesterov, M., Pleshakov, I., Fofanov, Ya. Information-physical properties of non-stationary responses in pulse signal processing systems, *Scientific Instrumentation*. 2006, vol. 16, no. 2, pp. 3-21.
34. Pleshakov, I.V., Popov, P.S., Dudkin, V.I., Kuzmin, Yu.I., Spin echo processor in functional electronic devices: Control of responses in processing of multipulse trains, *J. Commun. Technol. Electron.*, 2017, vol. 62, no. 6, pp. 583-587.
35. Pleshakov, I.V., Popov, P.S., Kuzmin, Yu.I., Dudkin, V.I., Multiplexing effect due to exposure of the working substance of a spin echo processor to magnetic field pulses, *Radiophysics and Quantum Electronics*, 2016, vol. 59, no. 2, pp. 161-168.
36. Rassvetalov, L.A. Comparative analysis of echo processors and alternative processing devices, *Proc. SPIE 3239, Photon Echo and Coherent Spectroscopy*, 1997, vol.3239, pp. 399-404.